

Supplementary Information

Carbon nanotube–DNA hybridized fluorescent sensor for sensitive and selective detection of mercury(II) ion

Libing Zhang, Tao Li, Bingling Li, Jing Li and Erkang Wang *

State Key Laboratory of Electroanalytical Chemistry, Changchun Institute of Applied Chemistry,

Chinese Academy of Sciences, Changchun, Jilin, 130022, P. R. China

Experimental Details.

Materials. The FAM-labeled ssDNA (5'-TTCTTTCTTCCCCTTGTTTGTT-FAM-3') was synthesized by Shanghai Sangon Biotechnology Co. Ltd. (Shanghai, China). The concentration of aptamer was determined using the 256 nm UV absorbance and the corresponding extinction coefficient. Single-walled carbon nanotubes were purchased from Shenzhen Nanotech Port Co. Ltd. (China). N,N-Dimethylformamide, anhydrous, 99.8% (DMF) and polyvinylpyrrolidone (PVP K-30) were purchased from Sigma-Aldrich (St. Louis, MO, USA). Metal ion solutions were prepared from nitrate salts. All the other chemicals were of analytical reagent grade and were used as received without further purification. Solutions were prepared with deionized water processed with a Milli-Q

ultra-high purity water system (Millipore, Bedford, MA, USA).

Instrumentation. UV-visible absorbance spectra were recorded on a Cary 500 scan UV-vis-NIR spectrophotometer (Varian, Harbor City, CA) at room temperature. Fluorescent emission spectra were recorded on a Perkin Elmer LS55 Luminescence Spectrometer (Perkin Elmer Instruments U.K.). A JASCO J-810 spectropolarimeter (Tokyo, Japan) was utilized to collect the circular dichroism (CD) spectra in the Tris-HCl buffer. The optical chamber (1 cm path length, 1 mL volume) was deoxygenated with dry purified nitrogen (99.99%) before use and kept the nitrogen atmosphere during experiments. The background of the buffer solution was subtracted from the CD data. Transmission electron microscopy (TEM) measurements were made on a TECNAI G2 (Philips, Holland) with an accelerating voltage of 200 kV.

Preparation of SWNTs. In the experiment, the SWNTs were treated by refluxing in 4.0 M HNO₃ for 24 h, the purpose is to remove the amorphous carbon, then were filtered with a 220 nm millipore size membrane with the aid of a pump and thoroughly washed with water to obtain a neutral state. Subsequently, the 3:1 concentrated H₂SO₄:HNO₃ mixture was chosen as the oxidizing acid in this cutting operation. The SWNTs were sonicated for 8 h in ice bath. Finally, they were filtered with a 220 nm millipore size membrane and dried under vacuum at 60 °C overnight.¹ The obtained SWNTs is about 5~9 nm in diameter and normally below 500 nm in length. In addition, typical TEM images of purified SWNTs are obtained, as shown in Fig S5.

Performance of Hg²⁺ Detection. The purified SWNTs were sonicated in DMF for

5 h to give a homogeneous black solution and stored for use. The working solution containing the FAM-labeled ssDNA was obtained by diluting the stock solution to a concentration of 100 nM using 20 mM tris-HCl buffer (100 mM NaCl, 5.0 mM KCl, pH 7.4). For Hg^{2+} assays, 50 μL of the ssDNA stock solution, appropriate concentrations of Hg^{2+} solution, and SWNTs solution as prepared were mixed and incubated for 20 min at room temperature, then the fluorescence intensity was measured.

Supplementary Figures

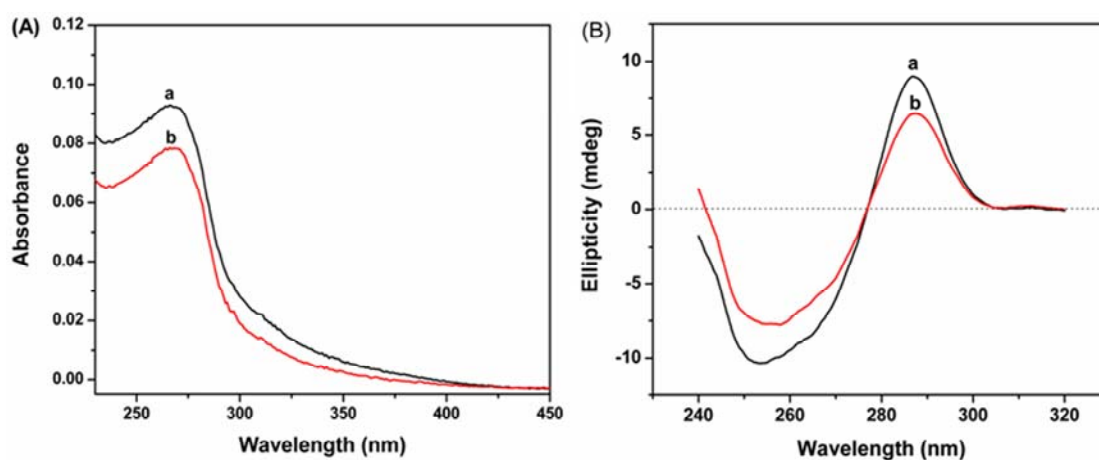


Fig. S1. (A) UV-visible absorbance spectra of ssDNA (100nM)/SWNTs (a) and ssDNA (100nM)/SWNTs + Hg^{2+} (b) in tris-HCl. (B) CD spectra of ssDNA (100nM) at different conditions: (a) ssDNA/SWNTs (40 $\mu\text{g}/\text{mL}$); (b) ssDNA/SWNTs (40 $\mu\text{g}/\text{mL}$) + Hg^{2+} (8.0 μM).

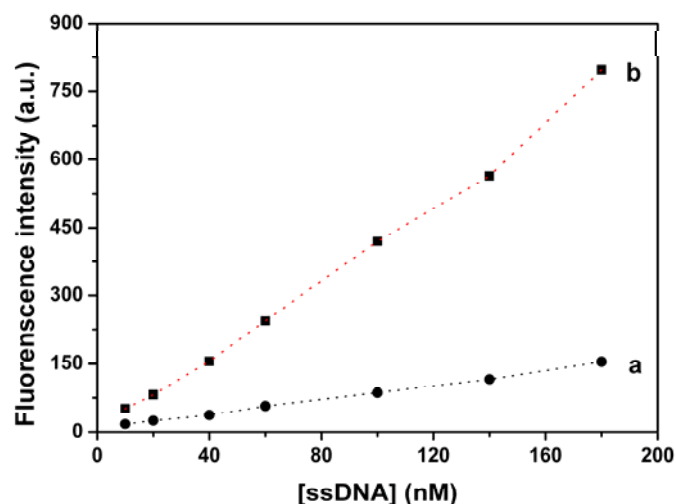


Fig. S2. Fluorescence emission intensity of ssDNA in the presence (a) and absence (b) of SWNTs in the ssDNA concentration range of 10–180 nM. Fluorescence intensity was recorded at 520 nm with an excitation wavelength of 480 nm.

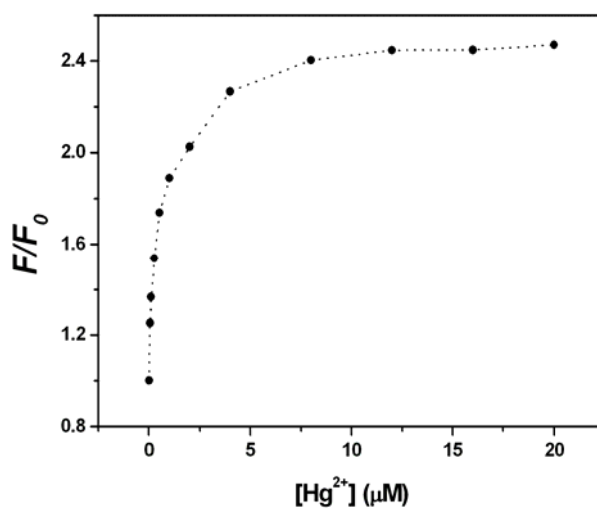


Fig. S3. Fluorescence enhancement of ssDNA/SWNTs in the tris-HCl buffer by increasing concentration of Hg²⁺ (0, 0.05, 0.1, 0.25, 0.5, 1.0, 2.0, 4.0, 8.0, 12.0, 16.0 and 20.0 μM). Fluorescence intensity was recorded at 520 nm with an excitation wavelength of 480 nm.

Fig. S4 shows the difference in fluorescence intensity between the blank and solutions containing Hg^{2+} or PVP. From the figure it is observed that, the fluorescence intensity enhanced with increasing the concentration of PVP, however even at a very large concentration of PVP, the fluorescence intensity is still much lower than the intensity of $4.0 \mu\text{M } \text{Hg}^{2+}$. This result indicates that PVP does not interfere with the detection of mercury.

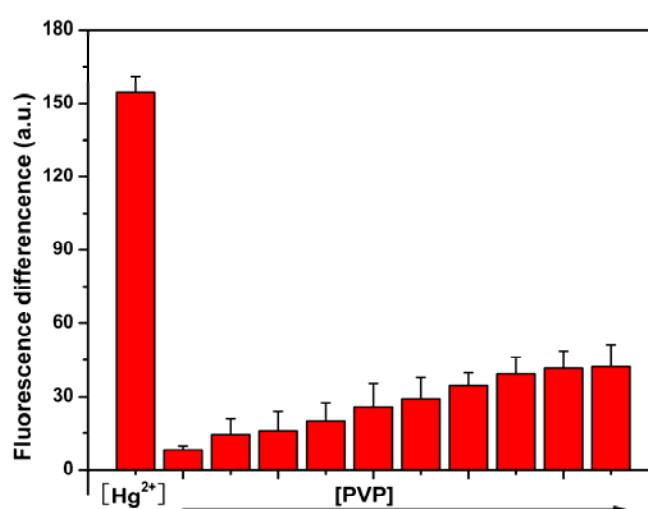


Fig. S4 The difference in fluorescence intensity between the blank and solutions containing Hg^{2+} or PVP. Concentration of Hg^{2+} is $4.0 \mu\text{M}$; concentration of PVP is 1.0 , 2.0, 3.0, 4.0, 5.0, 6.0, 7.0, 8.0, 9.0 and 10.0 mg/mL. Fluorescence intensity was recorded at 520 nm with an excitation wavelength of 480 nm.

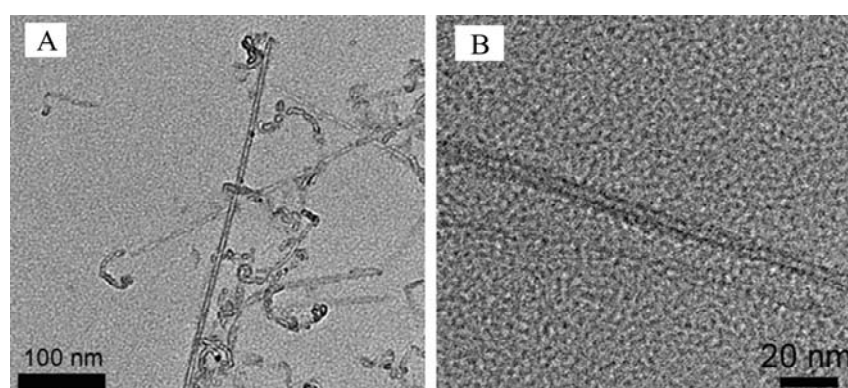


Fig. S5. TEM images of purified SWNTs.

Effect of Hg^{2+} Ions on the Fluorescence of ssDNA. Whether the fluorescence of ssDNA was greatly quenched with the increase of Hg^{2+} concentration. Fig. S6 shows the fluorescence emission spectrum of ssDNA in the presence of Hg^{2+} from 0 to 50.0 μM . No obvious emission change could be observed. The results demonstrate that the ssDNA/SWNTs approach could be used to detect Hg^{2+} in aqueous solution.

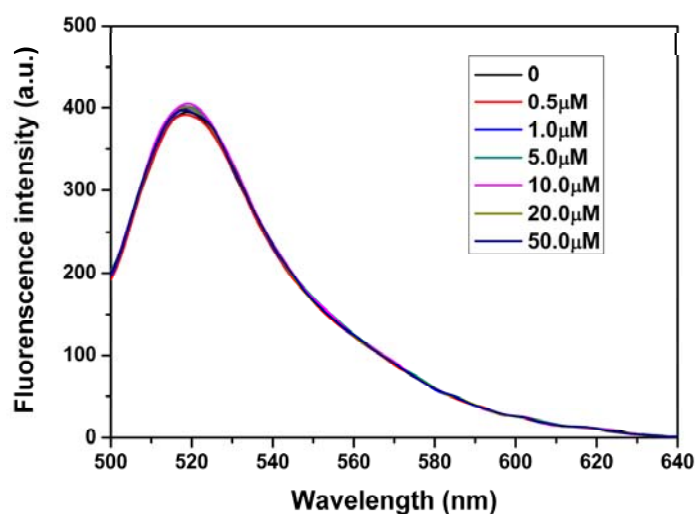


Fig. S6. Fluorescence emission spectra of ssDNA (50 nM) in the presence of different concentrations of Hg^{2+} from 0 to 50.0 μM . $\lambda_{\text{ex}} = 480$ nm.

The kinetic behavior. The kinetic behaviors of ssDNA /SWNTs in the absence and the presence of Hg^{2+} were studied. Fig. S7 shows fluorescence quenching of ssDNA as a function of incubation time. In the absence of Hg^{2+} , the curve exhibits a rapid reduction in the first 20 min and a slow decrease over a 40-min period. It is hypothesized that the surface effect of carbon nanotubes and the charge properties of ssDNA should be the main reason for the low adsorption.² In the presence of Hg^{2+} , a fluorescence decrease of ssDNA is also observed. However, the formation of dsDNA reduces the absorbance of ssDNA onto the SWNTs and thus fluorescence quenching efficiency. This, in turn, results in an overall fluorescence increase, which displays

fluorescence enhancement compared to that without Hg^{2+} . The experimental results demonstrate that the ssDNA/SWNTs approach could be used as a sensitive approach for Hg^{2+} detection in aqueous solution.

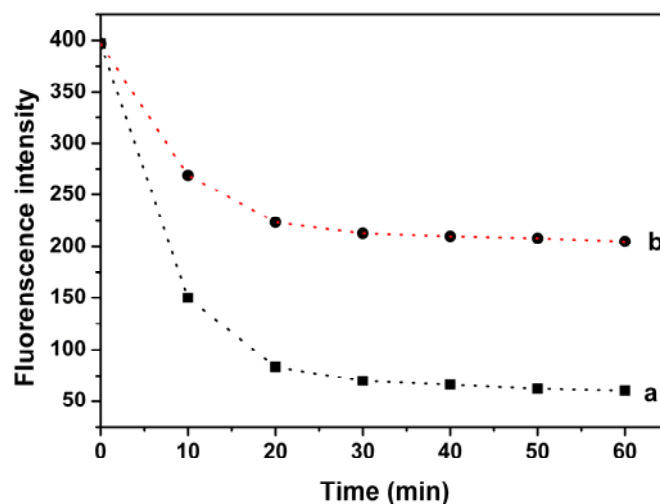


Fig. S7. Fluorescence quenching of ssDNA (100 nM) in tris-HCl by SWNTs as a function of time (a) in the absence of Hg^{2+} and (b) in the presence of Hg^{2+} of 4.0 μM . Fluorescence intensity was recorded at 520 nm with an excitation wavelength of 480 nm.

Optimization of the Variables of the Measuring System. The fluorescence response of the measuring system to Hg^{2+} was influenced by the acidity of the solution. Fig. S8 depicts the relationship between the fluorescence intensity ratio and pH from 4.0 to 12.0. The fluorescence intensity ratio of the system, F/F_0 , at $\lambda_{ex}/\lambda_{em} = 480 \text{ nm}/520 \text{ nm}$, increased with pH and reached a plateau when the pH is ~ 7.0 , where F_0 and F are FAM intensities at 520 nm in the absence and presence of Hg^{2+} , respectively. While at relatively higher pH (>8.0), the fluorescence intensity ratio of the system decreased gradually. It is obvious that the best F/F_0 response to pH in the range of 6.0–8.0. The result is in good agreement with the previous report.³ According

to the experimental result, we chose tris-HCl (pH 7.4) as buffer system in the experiment.

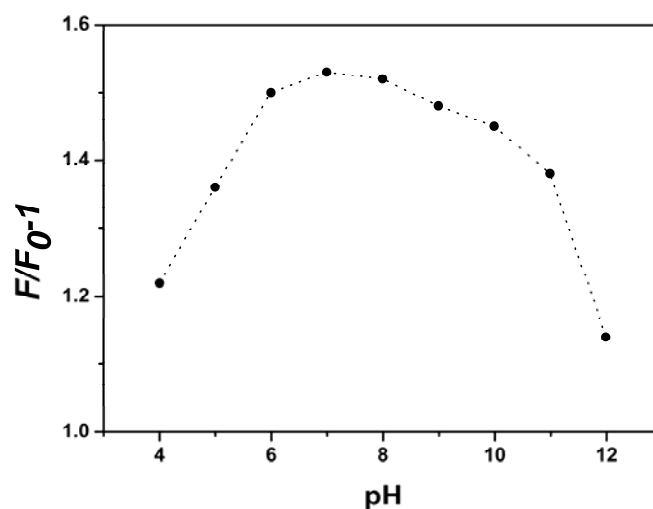


Fig. S8. Fluorescence intensity ratio of ssDNA/SWNTs as a function of pH, where F_0 and F are FAM intensities at 480/520 nm in the absence and presence of 4.0 μM Hg^{2+} , respectively.

The fluorescence response of ssDNA/SWNTs to Hg^{2+} is strongly dependent on the relative amount of ssDNA and SWNTs. It can be seen in the variation of the response sensitivity as a result of the different amount ratios of the ssDNA and SWNTs. Fig. S9 depicts the fluorescence intensity changes of ssDNA (100 nM) in the absence and presence of Hg^{2+} are plotted as a function of the concentration of SWNTs in tris-HCl buffer solution (pH 7.4). The fluorescence intensity of ssDNA is significantly decreased with increasing SWNTs concentration in the absence of Hg^{2+} (curve a). While in the presence of Hg^{2+} , Hg^{2+} can bind to the thymine-rich ssDNA, which changed the conformation of the ssDNA to form dsDNA. The formation of dsDNA will get away from SWNTs and thus increasing the fluorescence signal compared with

that without Hg^{2+} at the same conditions. Lower concentration of SWNTs results in the higher fluorescence recovery value in the system, but the blank fluorescence intensity is also high; while at relatively higher SWNTs concentration, the background fluorescence is low, but the fluorescence recovery is also decreased even if in a high Hg^{2+} concentration, accordingly, the response sensitivity will be reduced. The inset of Fig. S9 shows the relationship between the fluorescence intensity ratio (F/F_0) and the concentration of SWNTs, where F_0 and F are FAM intensities at 520 nm in the absence and presence of Hg^{2+} with an excitation wavelength of 480 nm. Obviously, it can be seen that the best response sensitivity emerged when the concentration of SWNTs was 10–12 mg/ml.

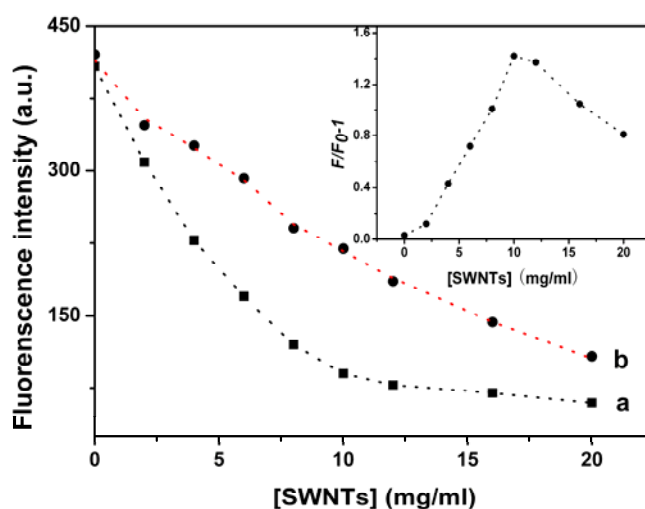


Fig. S9. Effect of SWNTs concentration on the fluorescence intensity of ssDNA (100 nM) in the absence (a) and the presence of 4.0 μM Hg^{2+} (b) in the tris-HCl buffer. Inset: the emission enhancement of ssDNA by 4.0 μM Hg^{2+} as a function of SWNTs concentration. Fluorescence intensity was recorded at 520 nm with an excitation wavelength of 480 nm.

Reference

1. (a) J. Liu, A. G. Rinzler, H. Dai, J. H. Hafner, R. K. Bradley, P. J. Boul, A. Lu, T. Iverson, K. Shelimov, C. B. Huffman, F. Rodriguez–Macias, Y.–S. Shon, T. R. Lee, D. T. Colbert and R. E. Smalley, *Science*, 1998, **280**, 1253. (b) J. Qu, Y. Shen, X. Qu and S. Dong, *Chem. Commun.*, 2004, 34.
2. (a) E. S. Jeng, A. E. Moll, A. C. Roy, J. B. Gastala, and M. S. Strano, *Nano Lett.*, 2006, **6**, 371.; (b) S. R. Vogel, M. M. Kappes, F. Henrich and C. Richert, *Chem. Eur. J.*, 2007, **13**, 1815.; (c) E. S. Jeng, P. W. Barone, J. D. Nelson and M. S. Strano, *Small*, 2007, **3**, 1602.
3. Y. Miyake, H. Togashi, M. Tashiro, H. Yamaguchi, S. Oda, M. Kudo, Y. Tanaka, Y. Kondo, R. Sawa, T. Fujimoto, T. Machinami and A. Ono, *J. Am. Chem. Soc.*, 2006, **128**, 2172.